

Photoinduced Desorption of Molecules from Metal Surfaces Using Femtosecond Pulses: A Model Dynamical Study

N. Chakrabarti,[†] N. Sathyamurthy,^{†,§} and J. W. Gadzuk^{*,‡}

Department of Chemistry, Indian Institute of Technology, Kanpur 208 016, India, and National Institute of Standards and Technology, Gaithersburg, Maryland 20899

Received: October 31, 1997

The influence of a femtosecond laser pulse on an adsorbate molecule–metal surface system is investigated by considering a time-dependent coupling between the ground- and excited-state potential energy curves using the time-dependent quantum mechanical wave packet approach. It is shown that the probability of desorption is strongly dependent on the duration of the coupling and the image–charge attraction and that it increases with increase in vibrational excitation of the metal–adsorbate bond.

1. Introduction

Photoinduced desorption (PID) of molecules from surfaces is being studied with renewed vigor because of the availability of femtosecond (fs) laser pulses.^{1–3} Early experiments by Cavanagh and co-workers⁴ on Pt(111)/NO and subsequent ones by Murata and co-workers⁵ using nanosecond (ns) laser pulses in the UV–visible region showed that the desorbed NO was translationally and rovibrationally hotter than could be accounted for by surface heating or other thermal relaxation processes. Further experiments on Pd(111)/NO,⁶ Ag(111)/NO,⁷ Cu(111)/NO,^{7,8} Pt(111)/O₂,⁹ and Cu(111)/CO¹⁰ using shorter laser pulses also yielded vibrationally hot desorbed molecules (NO, CO) and in some cases the yield (Y) increased nonlinearly with increase in laser fluence (LF).

Results on PID obtained using ns pulses could be accounted for by a two-state four-step model¹¹ in the spirit of Menzel–Gomer–Redhead (MGR)¹² and Antoniewicz¹³ models. The essential features of the proposed mechanism are the creation of hot electrons by the incident photon, formation of negative ions of adsorbate, and image–charge attraction to the surface resulting in neutralization and desorption. Holloway and co-workers¹⁴ included the electronic motion explicitly in a time-dependent quantum mechanical framework. Saalfrank et al. used a density matrix approach¹⁵ and also a wave packet approach¹⁶ to investigate the PID, in one dimension.

In our earlier work¹⁷ we had examined the possibility of photoinduced desorption in a model Pt–NO system by transferring the wave function corresponding to the ground electronic ground vibrational state of the substrate–adsorbate to the electronic excited-state potential energy surface (PES), which included an electron transfer from the metal to the molecule and the concomitant image–charge¹⁸ interaction. We had assumed a δ -function for the temporal structure of the excitation and had time-evolved the wave packet on the excited-state PES for various time intervals. By considering a δ -function deexcitation to the ground-state PES and time-evolving further, we could compute the desorption probability (P_{des}).¹⁹ As expected,

P_{des} was found to be a strong function of the residence time (Δt_d) on the excited-state PES. The experimentally observed P_{des} would correspond not to any particular Δt_d but to a distribution of Δt_d .

Understanding the experimental results obtained using fs pulses rather than ns pulses of equal fluence requires one to go beyond the two-state four-step model discussed above because the fs pulses generate a much larger number density of hot electrons. Under these conditions there is the likelihood of a manyfold repetition of the transfer events between the PES described above, now involving the adsorbate–substrate bond in various stages of vibrational excitation. This is referred to as DIMET²⁰ (desorption induced by *multiple* electronic transitions) in contrast to the DIET (desorption induced by electronic transition) mechanism proposed earlier.¹¹ There have also been related efforts to interpret the fs results explicitly in terms of electronic friction.²¹

In an attempt to better understand the fundamental quantum dynamics involved in the PID process, we focus attention here on the temporal shape of the pulse and its influence on the excitation dynamics of the adsorbate–substrate coordinate. Since the electronic motion is relatively fast, it should be adequate to concentrate on the nuclear motion as long as we have a reasonable representation of the coupling between the ground- and excited-state potential energy curves. We present a model study in which the time-dependent coupling is given a temporal shape proportional to that of the (fs) laser pulse. We then solve the coupled nuclear motion problem using time-dependent quantum mechanical wave packet propagation techniques.²² Such an approach allows for continuous transfer of the system wave function from the ground electronic state to the excited electronic state and back throughout the duration of the interaction. This procedure appears to be similar to a continuous limit of the discrete up-and-down cycling which is the defining characteristic of the DIMET process. Guo and Liu²³ have taken a similar view of the problem but followed the time-dependent perturbation theoretic route without taking into account an explicit time-dependence of the coupling.

The basic methodology and numerical details of our approach are presented in section 2. That is followed by a presentation of results and discussion in section 3 and summary and conclusion in section 4.

[†] Indian Institute of Technology.

[§] Honorary Professor, S. N. Bose National Centre for Basic Sciences, Calcutta, India.

[‡] National Institute of Standards and Technology.

TABLE 1: Potential Energy Parameters

D_e	1.08 eV
α	$1.708 a_0^{-1}$
Z_e	$2.83 a_0$
W	5.70 eV
EA	0.026 eV
δZ	$0.15 a_0$

2. Methodology

The photodesorption dynamics of an adsorbate–substrate system can be followed by solving the coupled time-dependent Schrödinger equation

$$i\hbar \frac{\partial}{\partial t} \begin{pmatrix} \psi_g \\ \psi_e \end{pmatrix} = \begin{pmatrix} H_g & V_{\text{int}} \\ V_{\text{int}} & H_e \end{pmatrix} \begin{pmatrix} \psi_g \\ \psi_e \end{pmatrix} \quad (1)$$

where ψ_g and ψ_e represent the wave functions in the ground and excited states, respectively. H_g is the ground-state Hamiltonian

$$H_g = -\frac{\hbar^2}{2M} \frac{\partial^2}{\partial Z^2} + V_g(Z) \quad (2)$$

where M is the mass of the desorbing molecule, Z the desorption coordinate, and V_g the ground-state potential energy (PE) curve. H_e is the excited-state Hamiltonian defined analogous to H_g , with V_e , the excited-state PE curve taking the place of V_g in eq 2. V_{int} represents the interaction between the ground and excited electronic states of the system. In the absence of any external influence, it would correspond to the nonadiabatic coupling in the diabatic representation and would be Z -dependent. In the present case, however, it would represent the consequences of the fs laser pulse interaction with the substrate–adsorbate system, which includes the creation of hot electrons and their interaction with the adsorbate. Since such an interaction would be strongly dependent on the shape of the laser pulse, it is not unreasonable, as an exploratory study, to allow V_{int} to be similar to the shape of the laser pulse.

As an illustrative example we consider

$$V_{\text{int}}(t) = A(t) \cos(\omega_p t) \quad (3)$$

where ω_p is the angular (central) frequency of the laser pulse. We choose

$$\begin{aligned} A(t) &= A_0 \sin^2(\pi t/t_p) \quad (0 \leq t \leq t_p) \\ &= 0 \quad (t < 0, t > t_p) \end{aligned} \quad (4)$$

where A_0 is proportional to the amplitude of the excitation pulse (taken to be unity) and t_p is its duration. Although other shapes such as a Gaussian could have been considered, we do not expect the results to be too strongly dependent on such finer details. In addition, the shape function described in eq 4 has a smooth switch-on-and-off behavior.²⁴

We have considered a Morse type of interaction between the metal surface and the center-of-mass of the adsorbate for the ground-state PE curve:

$$V_g = D_e [e^{-2\alpha(Z-Z_e)} - 2e^{-\alpha(Z-Z_e)}] \quad (5)$$

where D_e , α , and Z_e are the Morse parameters corresponding to Pt–NO interaction and are listed in Table 1. The excited-state PE curve, V_e , includes an image–charge interaction and a constant energy term (algebraic sum of the work function (W) for Pt(111) surface and the electron affinity (EA) of NO) to

TABLE 2: Choice of Z_{im} Values and the Corresponding Franck–Condon Energy Gaps (E_{exc}) and the Excitation Wavelengths (λ) for the Different Sets of Calculations

$Z_{\text{im}} (a_0)$	$E_{\text{exc}} (\text{eV})$	$\lambda (\text{nm})$
1.8	1.75	708
1.9	2.0	620
2.0	2.3	539
2.1	2.45	506

describe the state of the negative molecular ion and the positively charged surface, in addition to the Morse curve for the ground-state interaction with the well minimum shifted toward the metal surface by δZ :

$$V_e = D_e [e^{-2\alpha(Z-Z_e+\delta Z)} - 2e^{-\alpha(Z-Z_e+\delta Z)}] + (W - \text{EA}) - \frac{e^2}{4[Z_{\text{im}} + (Z - Z_e)]} \quad (6)$$

Values of W , EA, and δZ used are also included in Table 1. The value of Z_{im} is chosen differently in different sets of calculations (see below).

At $t = 0$ the wave function ψ_g corresponds to the Morse wave function (χ_v) for the vibrational state v of the ground electronic state and $\psi_e = 0$ (0 K approximation). Time evolution of the wave function on the coupled PE curves is followed numerically by solving eq 1 using the second-order differencing scheme:²⁵

$$\psi_g(t + \Delta t) = \psi_g(t - \Delta t) - \frac{2i\Delta t}{\hbar} H_g \psi_g(t) - \frac{2i\Delta t}{\hbar} V_{\text{int}}(t) \psi_e(t) \quad (7)$$

$$\psi_e(t + \Delta t) = \psi_e(t - \Delta t) - \frac{2i\Delta t}{\hbar} H_e \psi_e(t) - \frac{2i\Delta t}{\hbar} V_{\text{int}}(t) \psi_g(t) \quad (8)$$

Each time step Δt corresponds to 0.027 fs. The spatial propagation of the wave function is accomplished using the fast Fourier transform (FFT) algorithm. The spatial grid consisted of 1024 grid points with $(Z_{\text{min}}, \Delta Z, Z_{\text{max}}) = (2.0, 0.02, 22.46) a_0$.

Four different excited-state PE curves (characterized by four different image plane locations (Z_{im} values)) are considered, and for each one of them the excitation frequency corresponding to the Franck–Condon energy gap is chosen. The different values of Z_{im} used and the corresponding excitation wavelengths are mentioned in Table 2.

During the duration of the off-diagonal coupling, the dynamics is followed by solving eq 1. After the interaction is over, the time evolution of the wave function is carried out only on the ground-state PE curve. For calculating the desorption probability, P_{des} , we consider a separation point Z_d on the grid, beyond which the molecules are treated as desorbed. We have taken $Z_d = Z_e + 4a_0$ in our calculation. We have used a large enough grid (1024 grid points) to ensure that even after a long time evolution portions of the wave packet do not reach the grid edge and that P_{des} converges. At the end of the time evolution P_{des} is computed according to the following expression:

$$P_{\text{des}} = \int_{Z_d}^{Z_{\text{max}}} \psi(z, t_f) \psi^*(z, t_f) dz \quad (9)$$

where Z_{max} is the edge of the grid and $t_f \gg t_p$ is a final time when P_{des} has approached its asymptotic limit.

3. Results and Discussion

We consider the substrate–adsorbate system in its $v = 0$ state of the ground electronic state subjected to V_{int} defined in eq 3

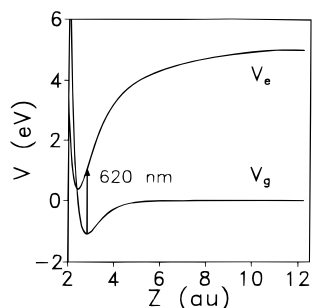


Figure 1. Potential energy curve for the ground and excited states of a model Pt-NO system for $Z_{\text{im}} = 1.9 a_0$. The Franck-Condon excitation wavelength is included.

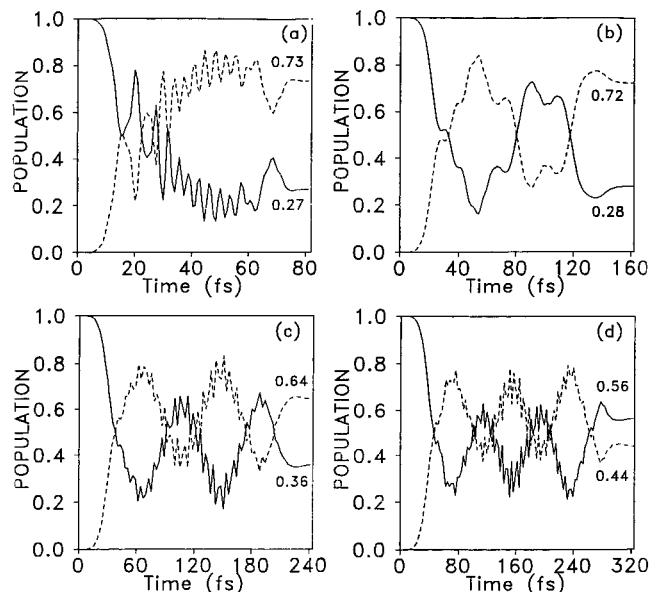


Figure 2. Population variation with time in the ground and excited states for V_{int} (eqs 3 and 4) with $t_p =$ (a) 80.80, (b) 161.62, (c) 242.44, and (d) 323.26 fs for initial $v = 0$ of the substrate-adsorbate coordinate. The solid line shows the population of the ground state and the dashed line that in the excited state.

with ω_p corresponding to $\lambda = 620$ nm. The excited-state PE is defined in eq 6 with $Z_{\text{im}} = 1.9 a_0$. The resulting PE curve, along with the ground-state PE curve, is illustrated in Figure 1. At $t = 0$, the wave function is located completely in the ground electronic state. With increase in time, more and more pieces of the wave function arrive in the excited state, while at the same time some of them get deexcited with the result that the population in the ground and excited states fluctuates with time,²⁶ as can be seen from Figure 2 for four different values of t_p (see eq 4). At the end of the time-dependent perturbation, population exchange between the states ceases and the populations on both the states become steady in the present model. To focus attention here on the desorption consequences due to the inherent time dependence of V_{int} , we have excluded any desorption from population trapped in the excited state that could subsequently decay into desorptive channels on the electronic ground state PE curve via other relaxation processes possibly operative in nature but not in our limited model. Thus the effective population that contributes to the (“stimulated” as opposed to “spontaneous”) desorption probability has arrived on the ground electronic state only as a result of V_{int} , and once this interaction is over, no further accumulation there is allowed. The resulting probability density distribution on the ground electronic state after the coupling is over is plotted in Figure 3

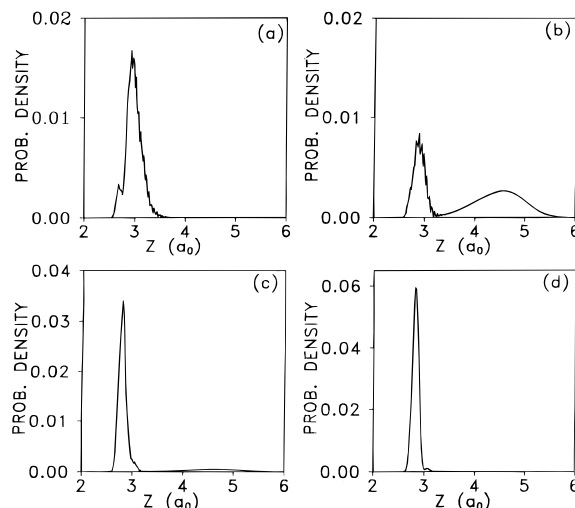


Figure 3. Probability density distribution on the ground electronic state (after the coupling is over) for different values of $t_p =$ (a) 80.80, (b) 161.62, (c) 242.44, and (d) 323.26 fs for initial $v = 0$ and $Z_{\text{im}} = 1.9 a_0$.

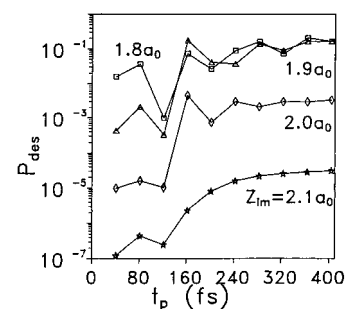


Figure 4. P_{des} as a function of t_p values for different Z_{im} values for initial $v = 0$.

for the different values of t_p . Values of P_{des} computed using eq 9 for four different excited states characterized by four different values of Z_{im} are plotted in Figure 4. It is seen that P_{des} is strongly dependent on the duration (t_p) of the coupling and also on the choice of Z_{im} . For Z_{im} values of 1.8, 1.9, 2.0, and 2.1 a_0 P_{des} varies over a wide range: 10^{-2} –0.20, 10^{-4} –0.16, 10^{-6} – 10^{-2} , and 10^{-4} – 10^{-7} , respectively. This is physically understandable since a smaller Z_{im} implies a larger force on the adsorbate while in the intermediate state and larger force would imply larger desorption probabilities. For a given Z_{im} , P_{des} increases in general with increase in t_p . However, there are local fluctuations in the curve and they correspond approximately to the vibrational period on the excited state (~ 60 fs).

As an illustrative example, for $Z_{\text{im}} = 1.9 a_0$ and $t_p = 80.80$ fs, we have examined the effect of vibrational excitation in the adsorbate-substrate mode on P_{des} . The results shown in Figure 5 indicate clearly that P_{des} increases with increase in v in keeping with the expectations of the DIMET mechanism.

Finally it is informative to put the present results into some perspective with past work in which the physical mechanism underlying the desorption process was modeled explicitly in terms of inelastic resonance scattering of hot electrons^{3,17,27} rather than implicitly in terms of a parametrized time-dependent trial function such as that given by eqs 3 and 4. As mentioned in the Introduction, the resonance scattering model presumed instantaneous transfer of wave function from the ground-to excited-state potential, propagation on the excited state for some time interval Δt_d , and then instantaneous return to the ground-state potential. To properly account for the probability of

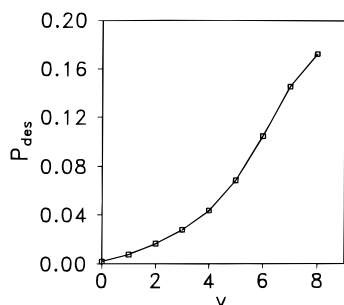


Figure 5. P_{des} values for different initial vibrational (v) states of the surface–adsorbate bond for $t_p = 80.80$ fs and $Z_{\text{im}} = 1.9 a_0$.

survival of the resonance state, the Δt_d -dependent desorption probability ($P_{\text{des}}(\Delta t_d)$) was averaged over all time intervals weighted by the exponential survival probability, resulting in the desorption probability that would be observed:

$$P_{\text{des}} = \langle P_{\text{des}}(\tau_R) \rangle = \frac{1}{\tau_R} \int_0^{\infty} d(\Delta t_d) e^{-\Delta t_d/\tau_R} P_{\text{des}}(\Delta t_d) \quad (10)$$

where τ_R is the mean lifetime of the temporary negative ion resonance state.²⁷ In effect, the “sudden-switching-with-exponential-averaging” procedure plays the role of a time-dependent coupling between ground and excited states in which the principal time-dependent feature is that the coupling is turned on for a time interval of order τ_R . The same job is fulfilled here by the envelope function $A(t)$ given by eq 4, where t_p substitutes for τ_R . It is for this reason that the desorption probability as a function of t_p (with various Z_{im} values) curves shown in Figure 4 here are qualitatively similar to the desorption probability versus τ_R curves presented elsewhere.²⁷ The consequence of the additional $\cos(\omega_p t)$ modulation of the off-diagonal interaction in eq 3 is most apparent as the “oscillatory fine structure” in the population versus time plots in Figure 2 and, as such, has only a secondary role in determining either the asymptotic long time population in either state or the ultimate desorption probabilities.

4. Summary and Conclusion

We have initiated an investigation of the influence of fs laser pulses on molecules adsorbed on metal surfaces by considering a time-dependent coupling between the ground and excited states of adsorbate–substrate interaction. We have considered a simple \sin^2 -shaped coupling and shown that the desorption probability, in general, increases with increase in the duration of the coupling. P_{des} increases with decreasing Z_{im} , for a given t_p . P_{des} increases with increasing vibrational excitation in the substrate–adsorbate coordinate, in keeping with the expectations of the DIMET mechanism.

Last, we have presented a narrative that demonstrates the complementary relation between the results of the present model

study and past desorption predictions based on the explicit physical mechanism of resonant inelastic scattering of energetic hot electrons.

Acknowledgment. This study was supported in part by a grant from the INDO-US subcommission. We are thankful to Dr. C. Kalyanaraman for his valuable assistance in some aspects of the study.

References and Notes

- (1) Zhu, X.-Y. *Annu. Rev. Phys. Chem.* **1994**, *45*, 113.
- (2) Zimmermann, F. M.; Ho, W. *Surf. Sci. Rep.* **1995**, *22*, 127. *Laser Spectroscopy and Photochemistry on Metal Surfaces*; Dai, H. L., Ho, W., Eds.; World Scientific: Singapore, 1995.
- (3) Gadzuk, J. W. In *Femtosecond Chemistry*; Manz, J., Wöste, L., Eds.; VCH Verlag: Weinheim, 1995; Chapter 20.
- (4) Buntin, S. A.; Richter, L. J.; Cavanagh, R. R.; King, D. S. *Phys. Rev. Lett.* **1988**, *61*, 1321. Buntin, S. A.; Richter, L. J.; Cavanagh, R. R.; King, D. S. *J. Chem. Phys.* **1989**, *91*, 6429. Cavanagh, R. R.; King, D. S.; Stephenson, J. C.; Heinz, T. F. *J. Phys. Chem.* **1993**, *97*, 786.
- (5) Peremans, A.; Fukutani, K.; Mase, K.; Murata, Y. *Surf. Sci.* **1993**, *283*, 189. Song, M.-B.; Suguri, M.; Fukutani, K.; Komori, F.; Murata, Y. *Appl. Surf. Sci.* **1994**, *79/80*, 25. Song, M.-B.; Mizuno, S.; Fukutani, K.; Murata, Y. *J. Chem. Phys. Lett.* **1992**, *196*, 559. Fukutani, K.; Song, M.-B.; Murata, Y. *Faraday Discuss.* **1993**, *96*, 105. Peremans, A.; Fukutani, K.; Mase, K.; Murata, Y. *Phys. Rev. B* **1993**, *47*, 4135. Fukutani, K.; Peremans, A.; Mase, K.; Murata, Y. *Surf. Sci.* **1993**, *283*, 158. Fukutani, K.; Peremans, A.; Mase, K.; Murata, Y. *Phys. Rev. B* **1993**, *47*, 4007.
- (6) Prybyla, J. A.; Heinz, T. F.; Misewich, J. A.; Loy, M. M. T.; Glowina, J. H. *Phys. Rev. Lett.* **1989**, *64*, 1537. Budde, F.; Heinz, T. F.; Loy, M. M. T.; Misewich, J. A.; de Rougemont, F.; Zacharias, H. *Phys. Rev. Lett.* **1991**, *66*, 3024.
- (7) So, S. K.; Franchy, R.; Ho, W. *J. Chem. Phys.* **1991**, *95*, 1385.
- (8) Kinoshita, I.; Misu, A.; Munakata, T. *J. Chem. Phys.* **1995**, *102*, 2970.
- (9) Kao, F.-J.; Busch, D. G.; Cohen, D.; Gomas da Costa, D.; Ho, W. *Phys. Rev. Lett.* **1993**, *71*, 2094.
- (10) Prybyla, J. A.; Tom, H. W. K.; Aumiller, G. D. *Phys. Rev. Lett.* **1988**, *68*, 503.
- (11) Gadzuk, J. W.; Richter, L. J.; Buntin, S. A.; King, D. S.; Cavanagh, R. R. *Surf. Sci.* **1990**, *235*, 317.
- (12) Menzel, D.; Gomer, R. *J. Chem. Phys.* **1964**, *41*, 3311. Redhead, P. A. *Can. J. Phys.* **1964**, *42*, 886.
- (13) Antoniewicz, P. R. *Phys. Rev. B* **1980**, *21*, 3811.
- (14) Harris, S. M.; Holloway, S.; Darling, G. R. *J. Chem. Phys.* **1995**, *102*, 8235.
- (15) Saalfrank, P.; Baer, R.; Kosloff, R. *Chem. Phys. Lett.* **1994**, *230*, 463.
- (16) Saalfrank, P. *Chem. Phys.* **1995**, *193*, 119.
- (17) Chakrabarti, N.; Balasubramanian, V.; Sathyamurthy, N.; Gadzuk, J. W. *Chem. Phys. Lett.* **1995**, *242*, 490.
- (18) Jennings, P. J.; Jones, R. O. *Adv. Phys.* **1988**, *37*, 341.
- (19) Because of an unfortunate interchange of mass factors for N and O, the excited-state PES used in the calculation differed slightly from that reported in ref 17 and as a result the P_{des} values reported therein in Figure 4a,b are overestimates. They should have been in the range 0–0.22. Alternatively, one could consider that P_{des} is sensitive to kinematic factors also.
- (20) Brandbyge, M.; Hedegard, P.; Heinz, T. F.; Misewich, J. A.; Newns, D. M. *Phys. Rev. B* **1995**, *52*, 6042.
- (21) J Head-Gordon, M.; Tully, J. C. *J. Chem. Phys.* **1995**, *103*, 10137.
- (22) Balakrishnan, N.; Kalyanaraman, C.; Sathyamurthy, N. *Phys. Rep.* **1997**, *280*, 79.
- (23) Guo, H.; Liu, L. *Surf. Sci.* **1997**, *372*, 337.
- (24) Manz, J. In *Femtochemistry and Femtobiology*; Sundström, V., Ed.; World Scientific: Singapore, 1997.
- (25) Tannor, D. J.; Rice, S. A. *Adv. Chem. Phys.* **1988**, *70*, 441.
- (26) Ramakrishna, M. V.; Coalson, R. D. *J. Chem. Phys.* **1988**, *120*, 327.
- (27) Gadzuk, J. W. *Phys. Rev. B* **1991**, *44*, 13466; *Surface Sci.* **1995**, *342*, 345; *Phys. Rev. Lett.* **1996**, *76*, 4234.